Supplementary Information

Two Luminescent Zn(II) Metal–Organic Frameworks For Exceptionally Selective Detection of picric acid explosive

Zhi-Qiang Shi,[ab] Zi-Jian Guo[a] and He-Gen Zheng*[a]

[a]*State Key Laboratory of Coordination Chemistry, School of Chemistry and Chemical Engineering, Collaborative Innovation Center of Advanced Microstructures, Nanjing University, Nanjing 210093, P. R. China*

[b]*College of Chemistry and Chemical Engineering, Taishan University, Taian 271021, P. R. China*

S1. Materials and general methods

All the chemicals and solvents purchased commercially and used without further purification. ^{1}H NMR spectra was measured on Bruker Avance 500 MHz with tetramethylsilane as the internal standard. Elemental analyses (C, H and N) were performed on a Perkin Elmer 240C elemental analyzer. IR (KBr pellet) spectra were recorded in the range of 4000–400 cm^{-1} on a Nicolet Impact 410 spectrometer using KBr pellets. Powder X-ray diffraction (PXRD) patterns were measured on a Bruker D8 Advance X-ray diffractometer using Cu-Kα radiation (λ = 1.5406 Å) at room temperature. Thermogravimetric analyses (TGA) were performed under nitrogen condition with a heating rate of 10 °C·min^{-1} using a Perkin Elmer thermogravimetric analyzer. Fluorescence spectra for the compounds were conducted with a SHIMAZU VF-320 X-ray fluorescence spectrophotometer at room temperature. UV-vis spectra were collected at room temperature using a Shimadzu UV-3600 double monochromator spectrophotometer.

S2. Photoluminescent sensing experiments

Finely ground sample of **MOF-1** or **MOF-2** (1 mg) was immersed in 2 mL corresponding pure organic solvents, respectively, treated by ultrasonication for 2 h, and then aged for 3 days to form stable suspensions before the fluorescence study. In the following nitro compounds sensing experiments, finely ground sample of **MOF-1** or **MOF-2** (1 mg) was immersed in 2 mL DMA to form stable suspension. The fluorescence was measured in-situ after incremental addition of freshly prepared analyte solutions (5 mM). The suspension was stirred at constant rate during experiment to maintain homogeneity.

S3. Synthesis of H_2L

The first step: A mixture of 2,5-dibromothiophene (2.42 g, 10 mmol), 3-ethoxycarbonylphenylboronic acid (5.82 g, 30 mmol), K_3PO_4 (12.74 g, 60 mmol), and $Pd(PPh_3)_4$ (1.16 g, 1 mmol) in dry 1,4-dioxane (200 mL) was heated to 100 °C for 3 days under N_2 atmosphere. After cooling to room temperature, solvent was removed by distillation under a vacuum. To the residue were added H_2O and $CHCl_3$, and the organic layer was extracted with $CHCl_3$ (200 mL × 3). The organic layer was dried by anhydrous $MgSO_4$ and filtered. Then the desired ester was separated by silica gel column chromatography (petroleum ether/dichloromethane = 2:1, v/v) to afford yellow powder in a yield 2.74 g (72%).

The second step: A mixture of the yellow carboxylic ester (1.91 g, 5 mmol), NaOH (3 g, 75 mmol), THF (50 mL), MeOH (50 mL) and H_2O (25 mL) was refluxed for 48 h. After cooling to room temperature, THF and MeOH were evaporated. Then the mixture was acidified with diluted HCl (1.0 $mol{\cdot}L^{-1}$) until no further precipitate was detected (pH ≈ 2-3). The yellow solid 3,3'-(thiophene-2,5-diyl)dibenzoic acid (H_2L) was collected by filtration in 87% yield after washing with water and drying in vacuum (1.41 g). ^{1}HNMR(500 MHz, DMSO): δ: 13.12 (s, 2H), 8.24 (s, 2H), 8.01 (d, 2H), 7.87 (d, 2H), 7.66 (s, 2H), 7.59 (t, 2H). IR(KBr, cm^{-1}): 3408(w), 1684(vs), 1602(w), 1581(m), 1448(m), 1418(m), 1308(s), 1260(m), 901(w), 786(w), 753(m), 708(w), 554(w). Anal. calcd for $C_{18}H_{12}O_4S$: C, 66.65%; H, 3.73%. Found: C, 66.58%; H, 3.79%; S, 9.97%.

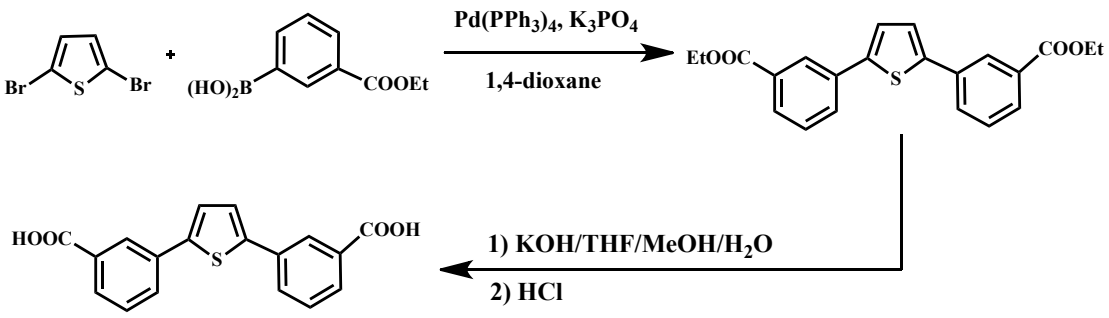

Scheme S1. Two-step synthesis route of H_2L.

S4. Synthesis of $[Zn_2(L)_2(dpyb)]$ (MOF-1) and $[Zn(L)(dipb)]\cdot 2H_2O$ (MOF-2)

A mixture of $Zn(NO_3)_2\cdot 6H_2O$ (14.9 mg, 0.05 mmol), H_2L (16.2 mg, 0.05 mmol), dpyb (5.8 mg, 0.025 mmol) was dissolved in 5ml of DMA/H_2O (2:3, v/v). The final mixture was transferred to a Parr Teflon-lined stainless steel vessel (15 mL) under autogenous pressure and heated at 85 °C for 3 days. Yellow block crystals of **MOF-1** were obtained. Yield: 45% (based on Zn). Anal. calcd for $C_{26}H_{15}NO_4SZn$: C, 62.10%; H, 3.01%; N, 2.79%. Found: C, 62.05%; H, 3.06%; N, 2.85%. IR(KBr, cm^{-1}): 3412(w),1634(vs), 1611(s), 1574(m), 1518(m), 1486(w), 1424(m), 1396(vs), 1221(w), 1074(w), 810(w), 764(m), 726(w), 4620(w). Light yellow block crystals of **MOF-2** were synthesized in the same condition except that dipb was added instead of dpyb. Yield: 38% (based on Zn). Anal. calcd for $C_{36}H_{28}N_4O_6SZn$: C, 60.89%; H, 3.97%; N, 7.89%. Found: C, 60.85%; H, 4.01%; N, 7.94%. IR(KBr, cm^{-1}): 3411(w), 1620(s), 1571(m), 1518(s), 1378(vs), 1308(m), 1264(m), 1126(w), 1066(m), 964(w), 817(m), 769(m), 687(w), 514(w).

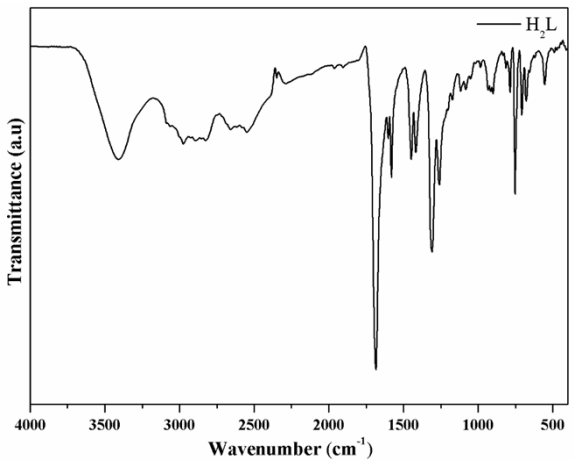

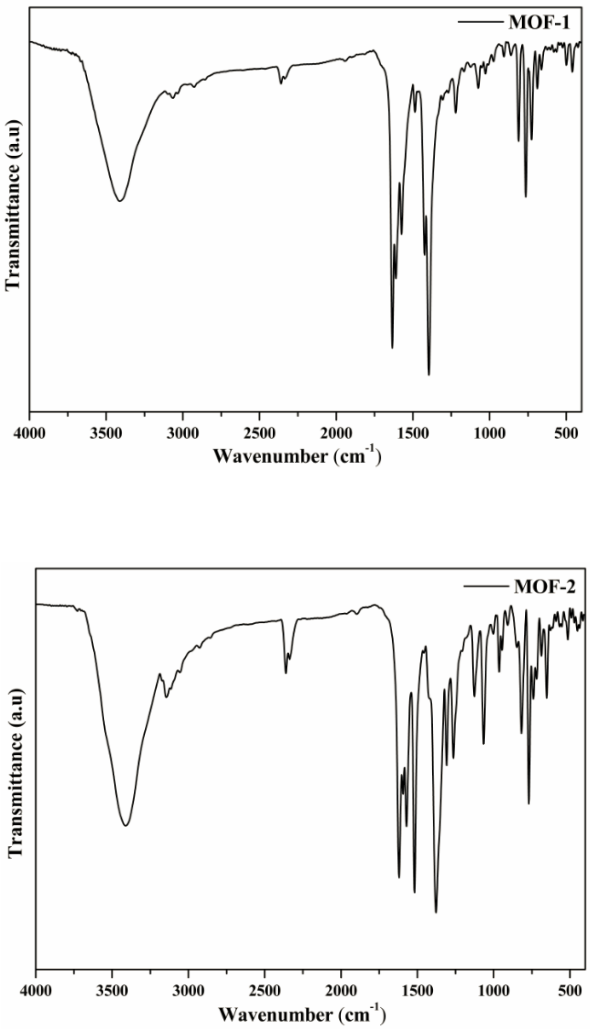

Fig. S1 IR spectra of H_2L, **MOF-1** and **MOF-2**.

S5. Single-crystal X-ray diffraction

Single crystal X-ray diffraction data for **MOF-1** and **MOF-2** were collected on a Bruker Smart Apex II CCD diffractometer using Mo Kα radiation (λ = 0.71073 Å). A semiempirical absorption correction was applied using SADABS program.[1] The structures were solved by direct methods and all non-hydrogen atoms were located from the trial structures and then refined anisotropically on F^2 refined by full-matrix least-squares procedures technique using the SHELXTL[1] crystallographic software package. The organic hydrogen atoms were generated geometrically. Guest solvent water molecules in the crystal of **MOF-2** were chemically featureless to refine using conventional discrete-atom models. Therefore the SQUEEZE program implemented in PLATON[2] was used to remove these electron densities. The detailed crystallographic data and structure refinement parameters are listed in Table S1. The selected bond lengths are given in Tables S2.

CCDC reference numbers of crystals **MOF-1** and **MOF-2** are 1035800 and 1035802, respectively.

Topological analyses were performed using the program package TOPOS.[3]

Table S1. Crystallographic Data and Structure Refinement Details for **MOF-1** and **MOF-2**.

Compound	**MOF-1**	**MOF-2**
Formula	$C_{26}H_{15}NO_4SZn$	$C_{36}H_{28}N_4O_6SZn$
Formula weight	502.82	710.10
Crystal system	Triclinic	Orthorhombic
Space group	*P* -1	*P*bca
a (Å)	7.9902(17)	18.3790(19)
b (Å)	11.043(2)	10.6606(11)
c (Å)	13.430(4)	31.736(3)
α (deg)	105.463(6)	90
β (deg)	102.922(6)	90
γ (deg)	107.508(4	90
V (Å^3)	1028.0(4)	6218.1(11)
Z	2	8
D_{calcd}(g cm^{-3})	1.624	1.440
μ(Mo Ka)(mm^{-1})	1.333	0.904
F(000)	512	2768
Temperature (K)	296(2)	296(2)
θ min-max (deg)	2.07, 25.05	1.28, 25.05
Tot., uniq. data	5395, 3559	32754, 5488
R(int)	0.0312	0.0571
Observed data [$I > 2\sigma(I)$]	2758	4350
N_{ref}, N_{par}	3559, 298	5488, 415
R_1[a],wR_2[b]($I > 2\sigma(I)$)	0.0446, 0.1089	0.0512, 0.1629
R_1,wR_2 (all data)	0.0668, 0.1249	0.0647, 0.1735
S	1.034	1.085
Min. and max resd dens (e·Å^{-3})	0.5392, -0.546	0.951, -0.831

[a] $R_1 = \Sigma||F_0|-|F_c||/\Sigma|F_0|$, [b] $wR_2 = \Sigma[w(F_0^2-F_c^2)^2]/\Sigma[w(F_0^2)^2]^{1/2}$.

Table S2. Selected Bond Lengths (Å) and Angles (deg) for **MOF-1** and **MOF-2**.

MOF- 1			
Zn(1)-O(2)	2.034(3)	Zn(1)-N(1)	2.061(3)
Zn(1)-O(4)#1	2.038(3)	Zn(1)-O(1)#2	2.063(3)
Zn(1)-O(3)#3	2.057(3)		
O(2)-Zn(1)-N(1)	101.19(13)	O(2)-Zn(1)-O(4)#1	88.39(14)
O(4)#2-Zn(1)-N(1)	104.31(13)	O(4)#1-Zn(1)-O(1)#2	89.95(14)
O(4)#2-Zn(1)-O(3)#3	158.78(12)	O(2)-Zn(1)-O(1)#2	159.06(12)
N(1)-Zn(1)-O(1)#2	99.45(13)	O(2)-Zn(1)-O(3)#3	86.31(13)
O(3)#3-Zn(1)-N(1)	96.88(13)	O(3)#3-Zn(1)-O(1)#2	87.74(13)
Symmetry codes: #1 = *x*, *y*, -1+*z*; #2 = 1-*x*, 1-*y*, -*z*; #3 = 1-*x*, 1-*y*, 1-*z*.			
MOF-2			
Zn(1)-O(1)	1.962(2)	Zn(1)-N(1)	2.001(3)
Zn(1)-N(3)#1	2.014(3)	Zn(1)-O(3)#2	1.977(3)
O(1)-Zn(1)-N(1)	111.04(12)	O(3)#2-Zn(1)-N(1)	106.39(12)
O(1)-Zn(1)-N(3)#1	96.85(12)	O(3)#2-Zn(1)-N(3)#1	121.52(13)
N(1)-Zn(1)-N(3)#1	109.06(13)		
Symmetry codes: #1 = *x*, 0.5-*y*, -0.5+*z*; #2 = 0.5+*x*, 1.5-*y*, -*z*.			

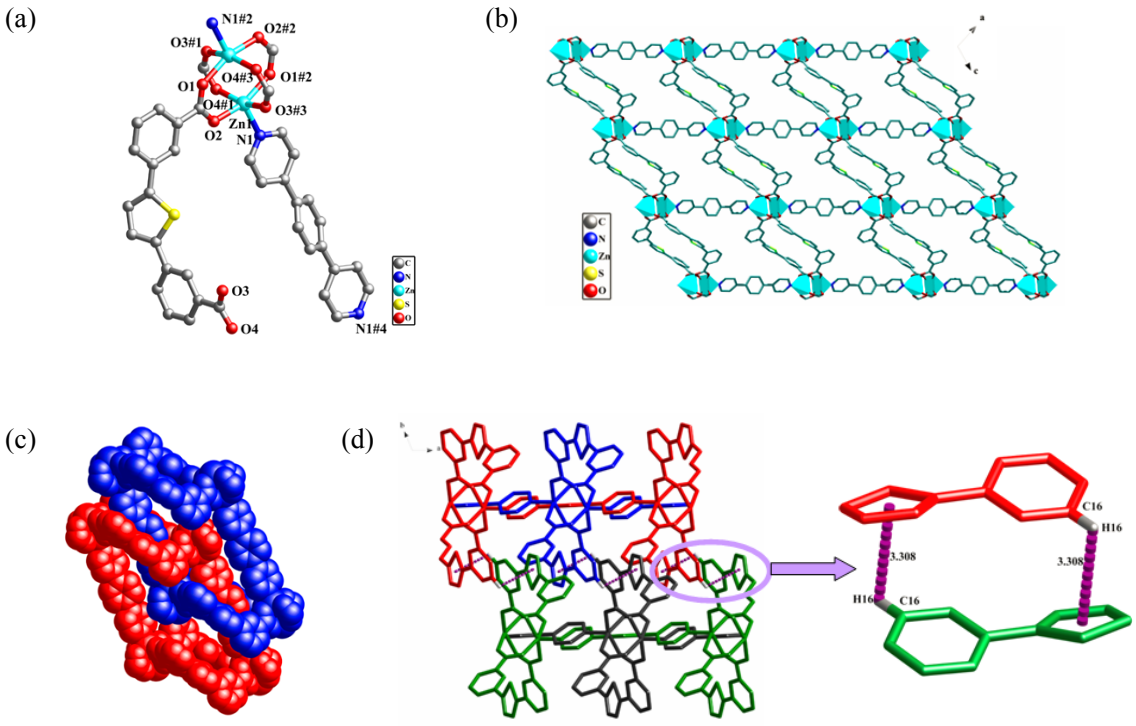

Fig. S2 (a) Coordination environment of the Zn(II) cation in **MOF-1**. The hydrogen atoms are omitted for clarity. Symmetry codes: #1 = *x*, *y*, -1+*z*; #2 = 1-*x*, 1-*y*, -*z*; #3 = 1-*x*, 1-*y*, 1-*z*; #4 = 3-*x*, 1-*y*, 1-*z*. (b) The 2D network of **MOF-1**. (c) Schematic representation of rotaxane unit. (d) Schematic representation of the 3D framework of **MOF-1**. The C–H···π interactions are shown with purple dash lines.

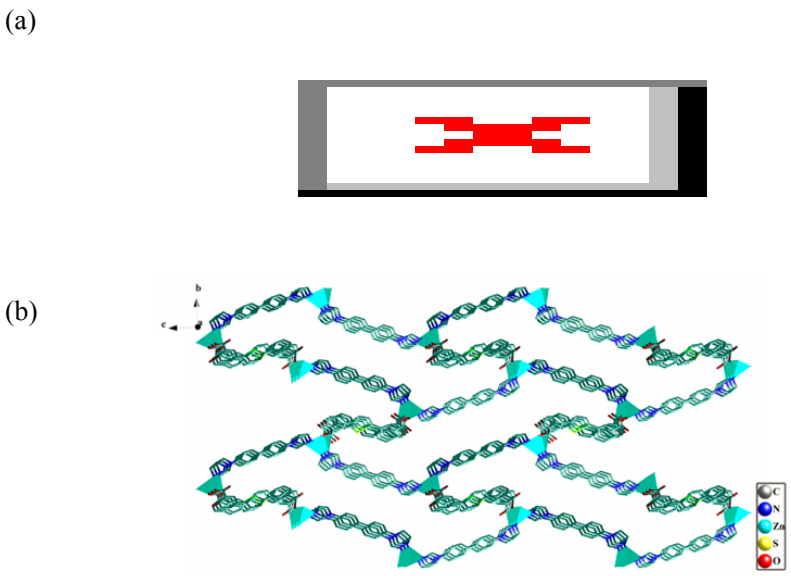

Fig. S3 (a) Coordination environment of the Zn(II) cation in **MOF-2**. The hydrogen atoms are omitted for clarity. Symmetry codes: #1 = *x*, 0.5-*y*, -0.5+*z*; #2 = 0.5+*x*, 1.5-*y*, -*z*. (b) The 3D framework of **MOF-2**.

S6. PXRD and thermal analysis

Powder X-ray diffractions (PXRD) experiments were carried out for **MOF-1** and **MOF-2** at room temperature to characterize their purity, as shown in Fig.s S2 (ESI†). The measured peak positions are in agreement with the simulated peak positions, indicating of pure products.

Furthermore, thermo gravimetric analysis (TGA) experiments were carried out to characterize the thermal stability of **MOF-1** and **MOF-2** (Fig. S3). For **MOF-1**, the framework exhibits a thermal stability up to 412 °C and then undergoes a continuous weight loss attributed to the decomposition of the organic ligands. For **MOF-2**, the first weight loss of 5.37% (calcd 5.07%) from room temperature to 232 °C corresponds to the loss of two lattice water molecules. The second weight loss from 322 to 631 °C can be ascribed to the departure of organic ligands. The final residue maybe ZnO (obsd, 11.86%; calcd, 11.46%).

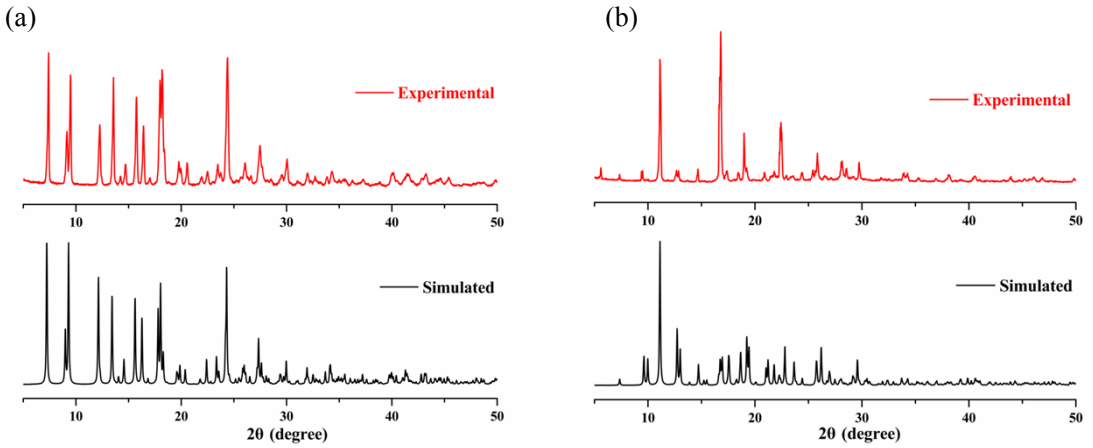

Fig. S4 Powder X-ray diffraction patterns of **MOF-1** (a) and **MOF-2** (b).

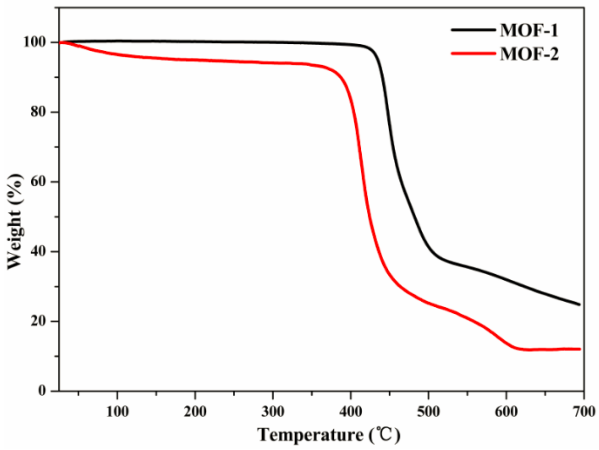

Fig. S5. TGA curves of **MOF-1** and **MOF-2**.

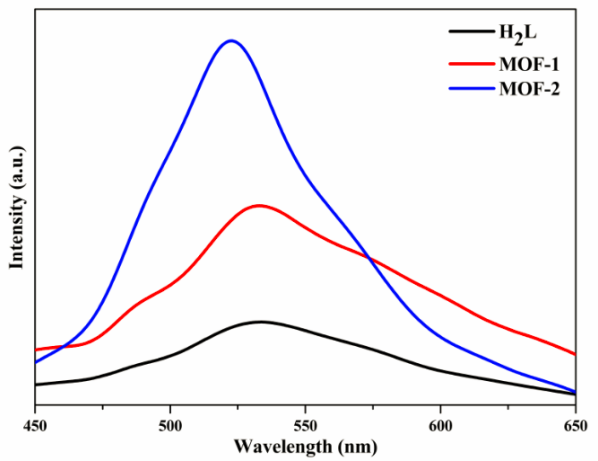

Fig. S6 Solid-state photoluminescent spectra of **MOF-1**, **MOF-2** and free H_2L ligand at room temperature when excited at 382 nm, respectively

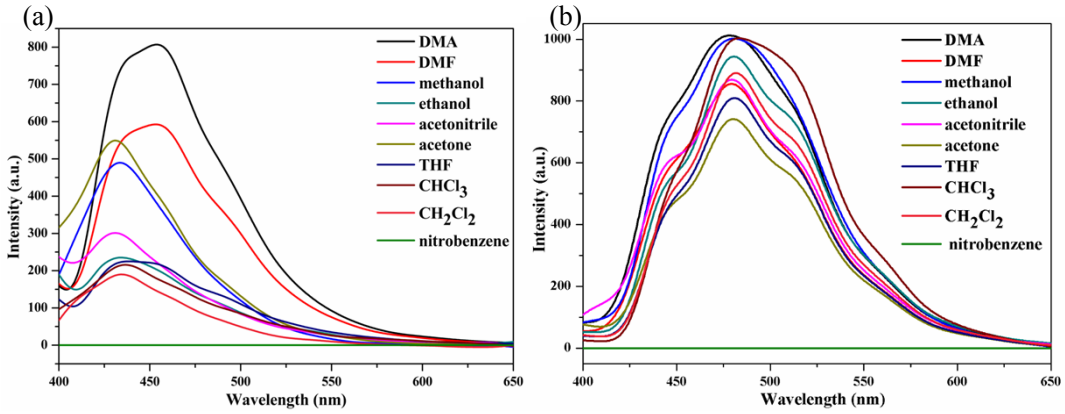

Fig. S7 Photoluminescent spectra of **MOF-1** (a) and **MOF-2** (b) in different solvents when excited at 382 nm, respectively.

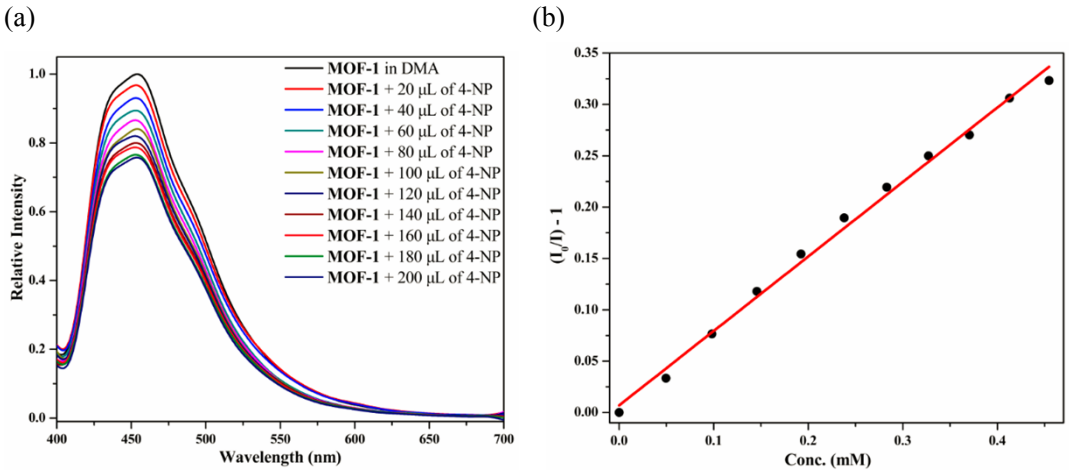

Fig. S8 Photoluminescent spectra (a) and SV plot (b) of **MOF-1** by gradual addition of 5 mM 4-NP in DMA.

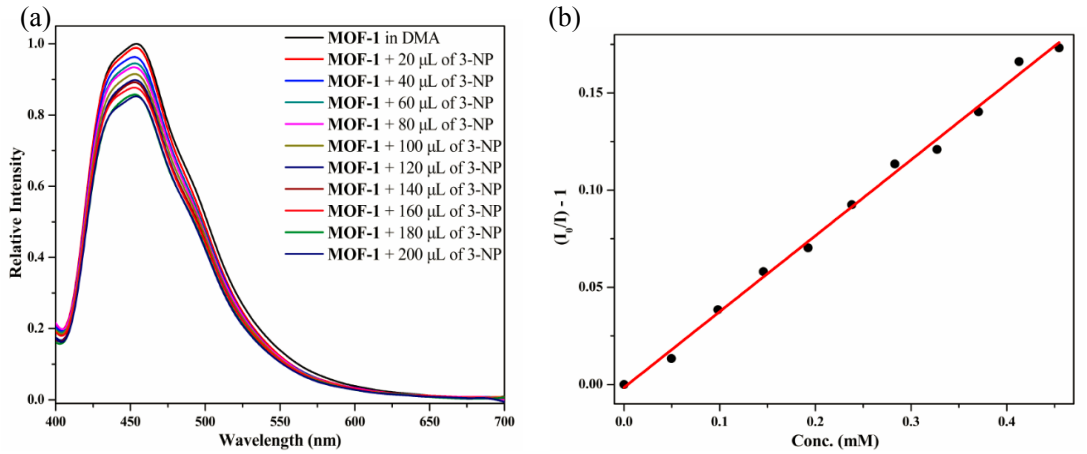

Fig. S9 Photoluminescent spectra (a) and SV plot (b) of **MOF-1** by gradual addition of 5 mM 3-NP in DMA.

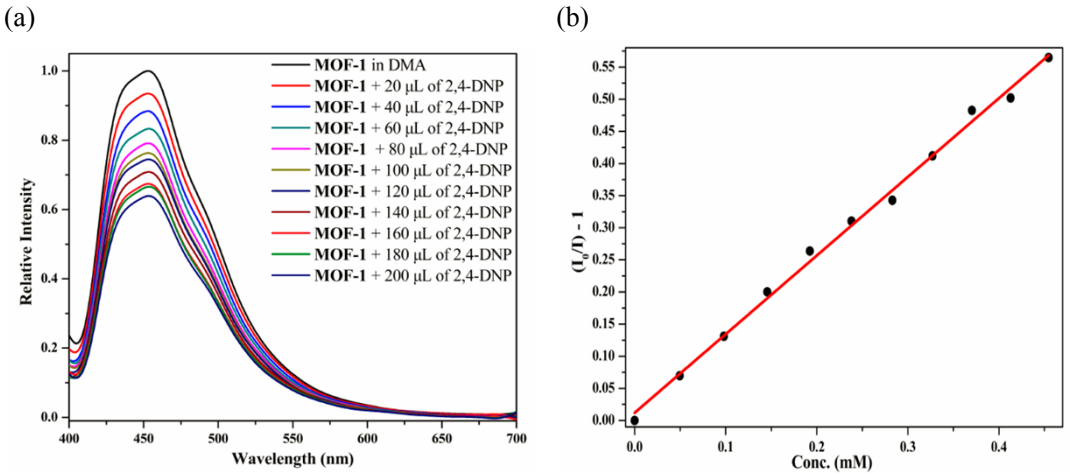

Fig. S10 Photoluminescent spectra (a) and SV plot (b) of **MOF-1** by gradual addition of 5 mM 2,4-DNP in DMA.

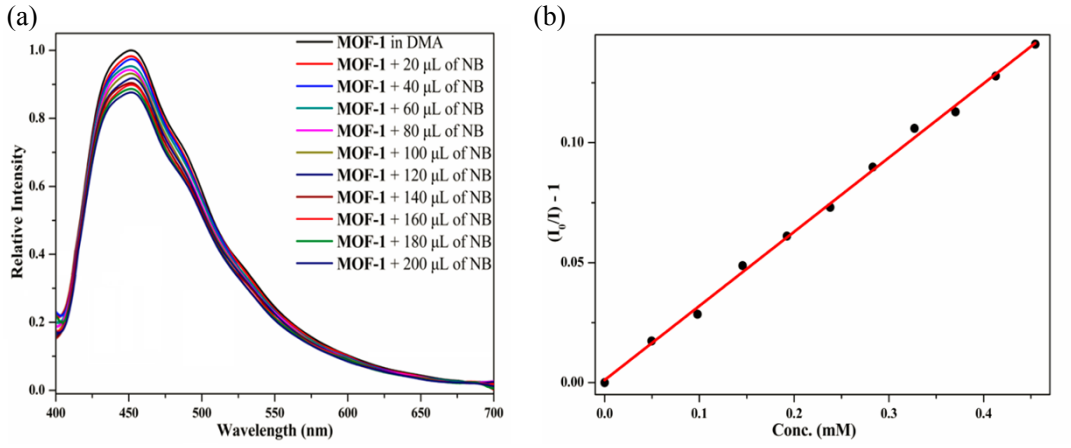

Fig. S11 Photoluminescent spectra (a) and SV plot (b) of **MOF-1** by gradual addition of 5 mM NB in DMA.

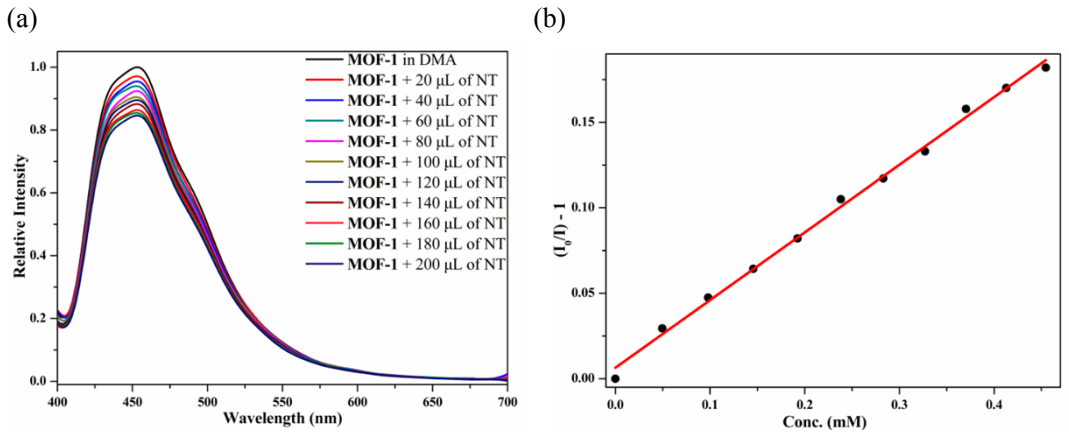

Fig. S12 Photoluminescent spectra (a) and SV plot (b) of **MOF-1** by gradual addition of 5 mM NT in DMA.

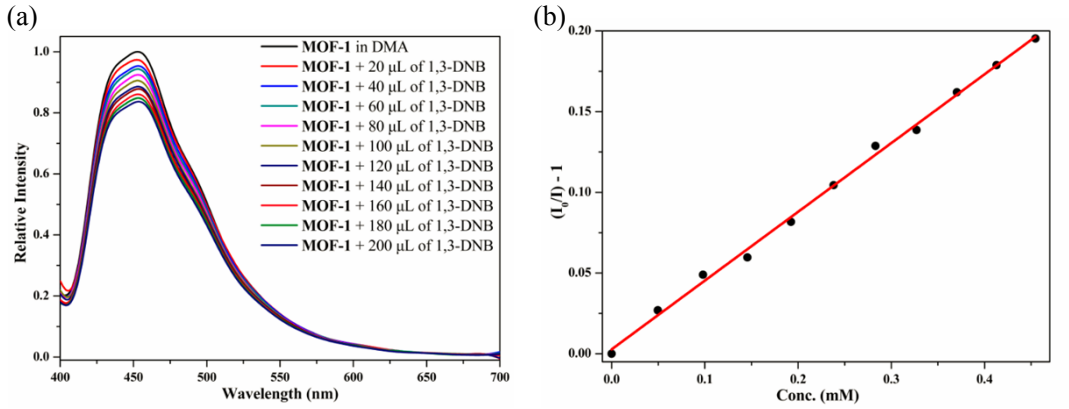

Fig. S13 Photoluminescent spectra (a) and SV plot (b) of **MOF-1** by gradual addition of 5 mM 1,3-DNB in DMA.

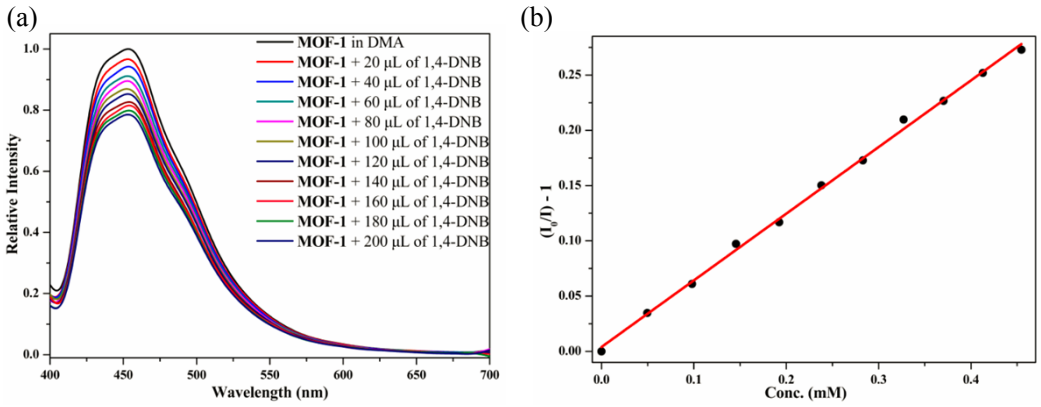

Fig. S14 Photoluminescent spectra (a) and SV plot (b) of **MOF-1** by gradual addition of 5 mM 1,4-DNB in DMA.

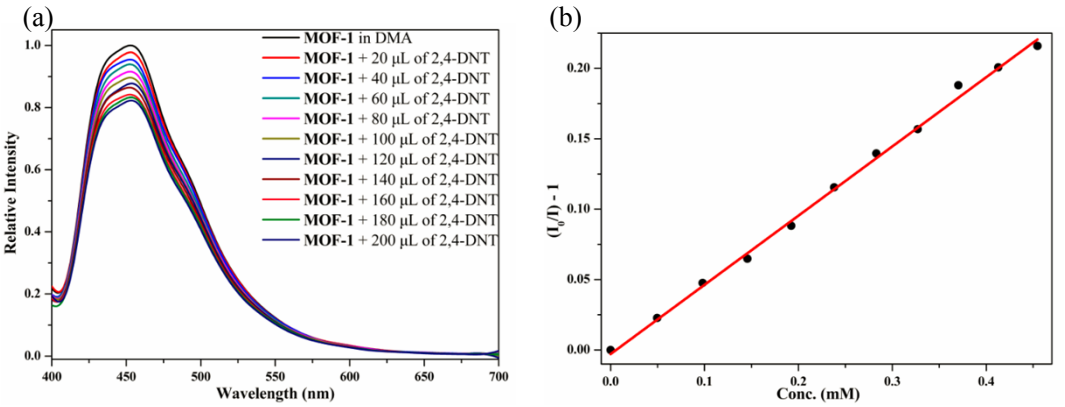

Fig. S15 Photoluminescent spectra (a) and SV plot (b) of **MOF-1** by gradual addition of 5 mM 2,4-DNT in DMA.

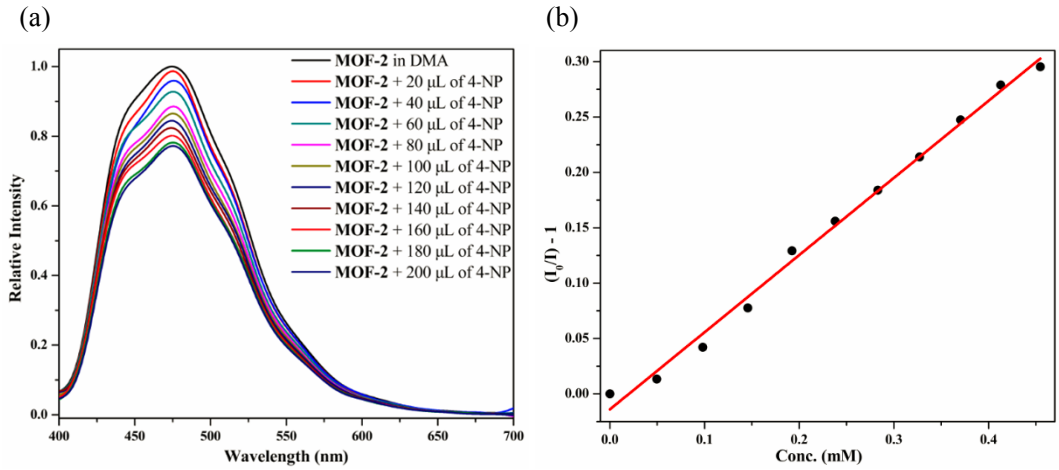

Fig. S16 Photoluminescent spectra (a) and SV plot (b) of **MOF-2** by gradual addition of 5 mM 4-NP in DMA.

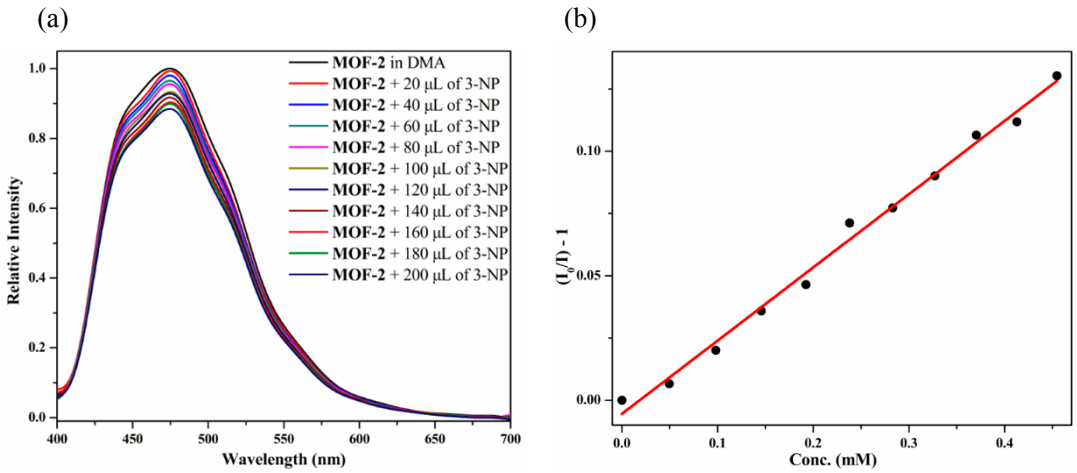

Fig. S17 Photoluminescent spectra (a) and SV plot (b) of **MOF-2** by gradual addition of 5 mM 3-NP in DMA.

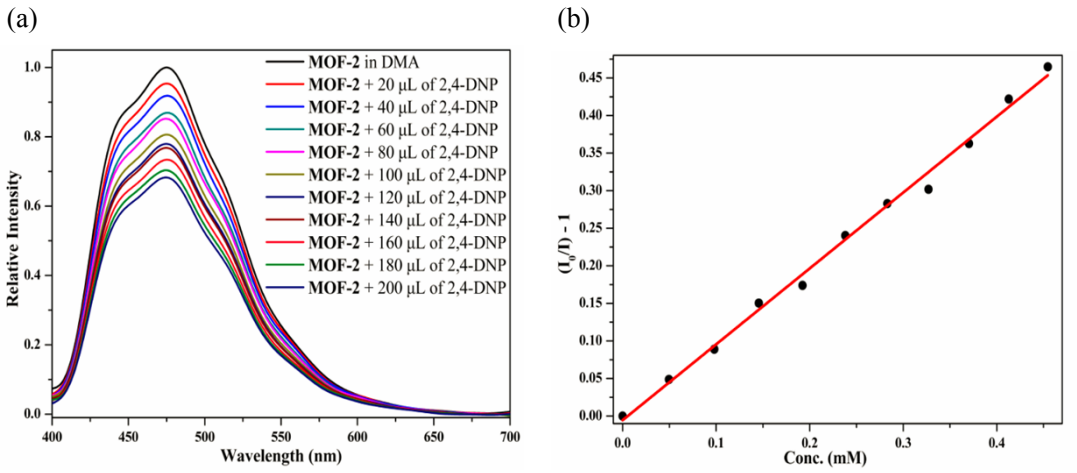

Fig. S18 Photoluminescent spectra (a) and SV plot (b) of **MOF-2** by gradual addition of 5 mM 2,4-DNP in DMA.

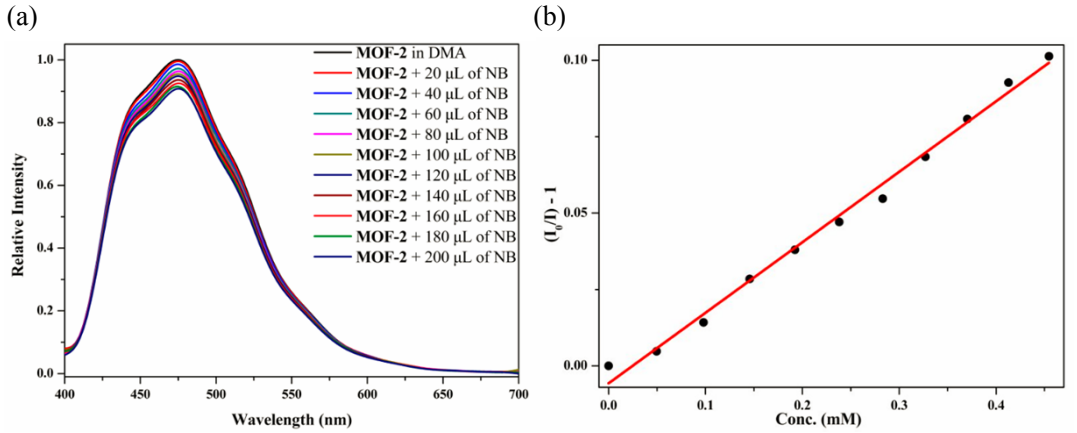

Fig. S19 Photoluminescent spectra (a) and SV plot (b) of **MOF-2** by gradual addition of 5 mM NB in DMA.

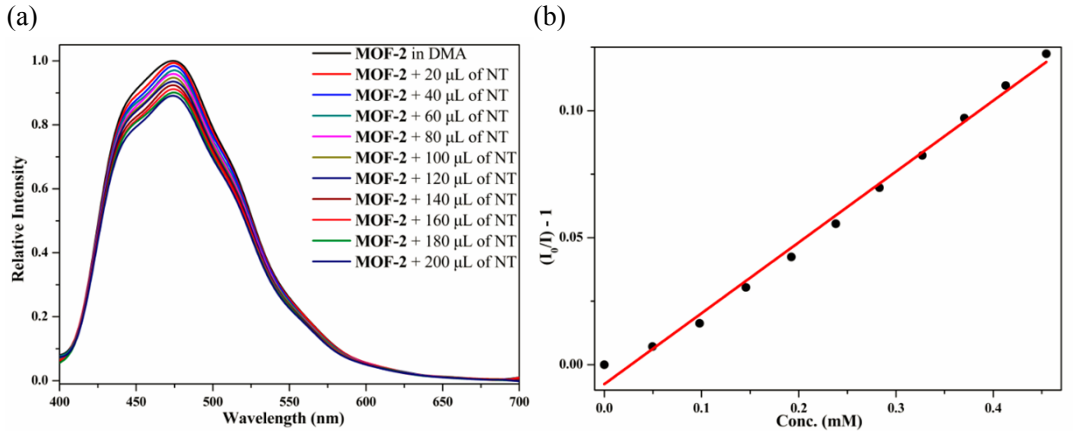

Fig. S20 Photoluminescent spectra (a) and SV plot (b) of **MOF-2** by gradual addition of 5 mM NT in DMA.

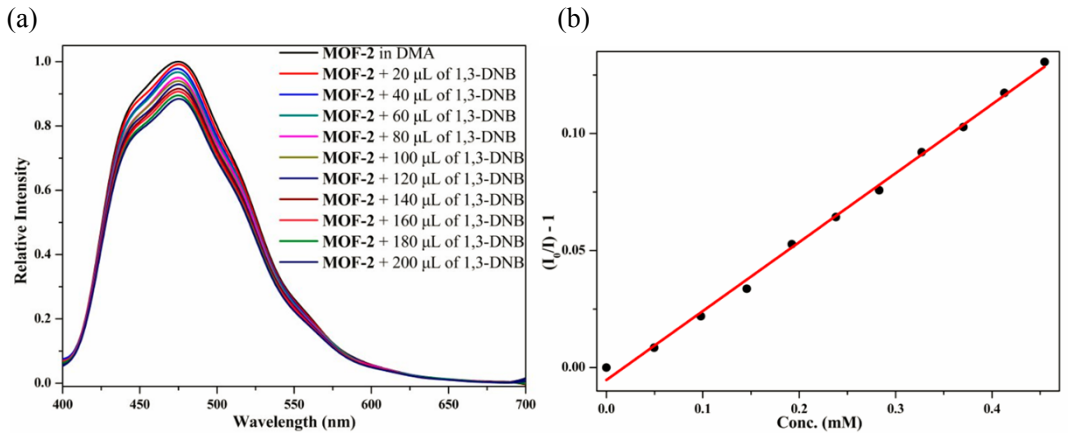

Fig. S21 Photoluminescent spectra (a) and SV plot (b) of **MOF-2** by gradual addition of 5 mM 1,3-DNB in DMA.

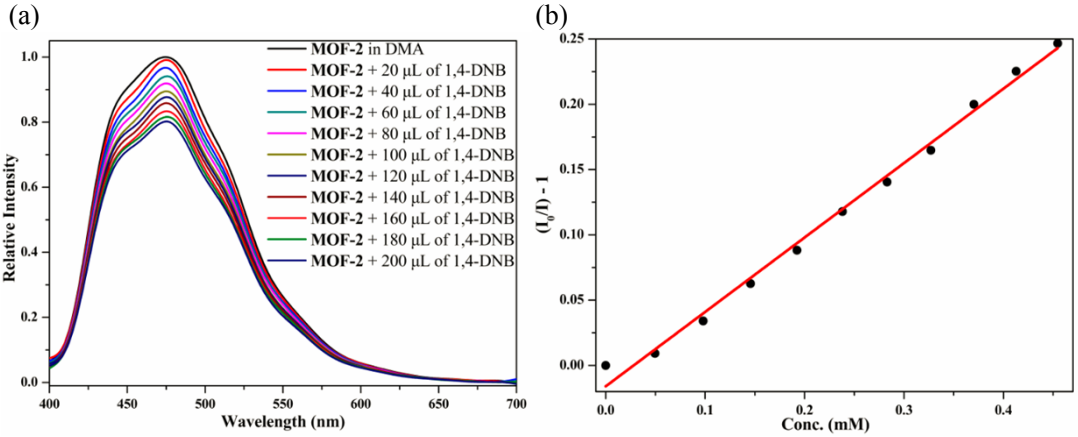

Fig. S22 Photoluminescent spectra (a) and SV plot (b) of **MOF-2** by gradual addition of 5 mM 1,4-DNB in DMA.

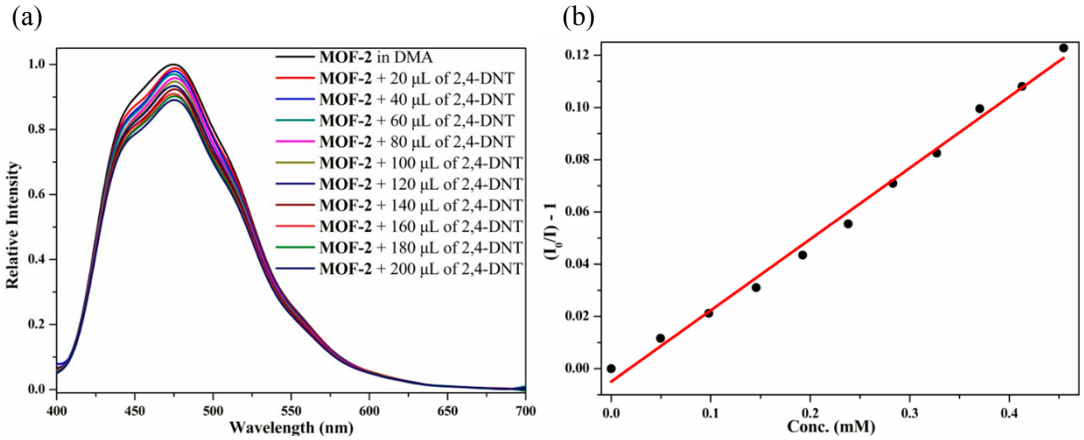

Fig. S23 Photoluminescent spectra (a) and SV plot (b) of **MOF-2** by gradual addition of 5 mM 2,4-DNT in DMA.

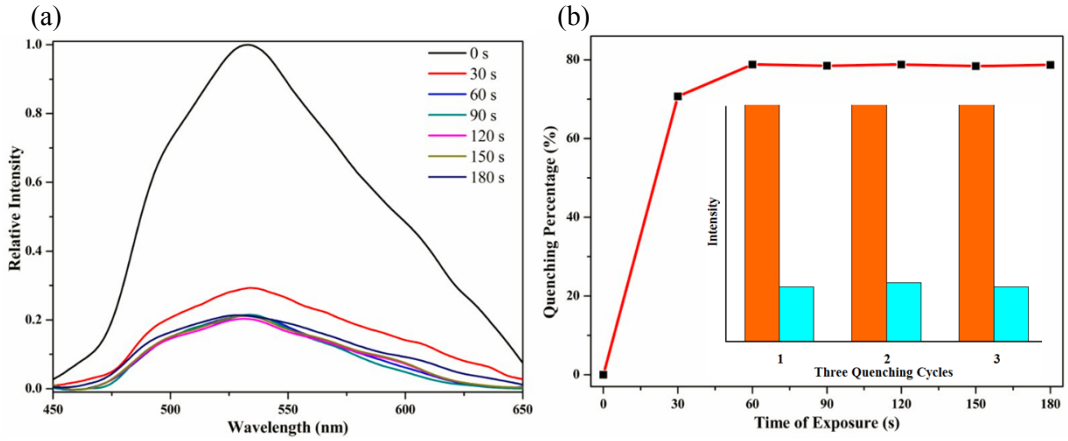

Fig. S24 (a) Time-dependent emission spectra after exposure of **MOF-1** to the PA vapor. (b) Fluorescence quenching percentage as a function of time by PA vapour. Inset: the results for three continuous quenching cycles.

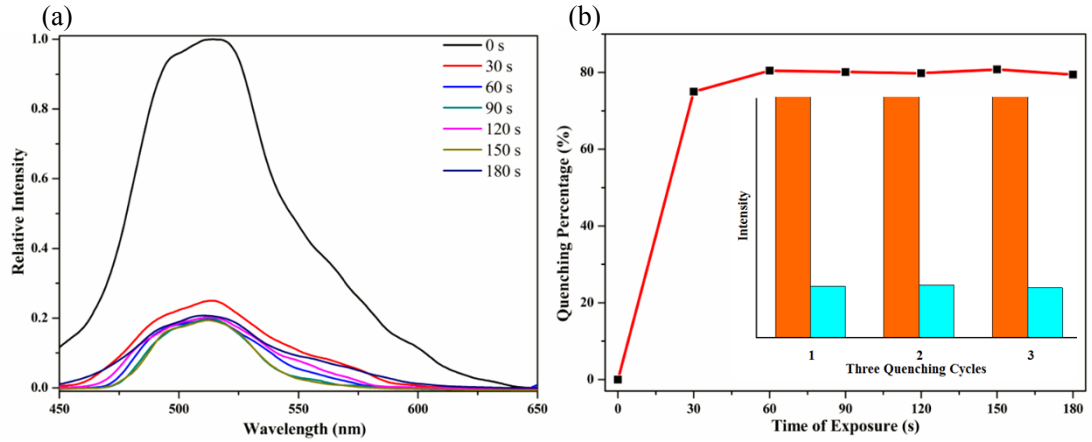

Fig. S25 (a) Time-dependent emission spectra after exposure of **MOF-2** to the PA vapor. (b) Fluorescence quenching percentage as a function of time by PA vapour. Inset: the results for three continuous quenching cycles.

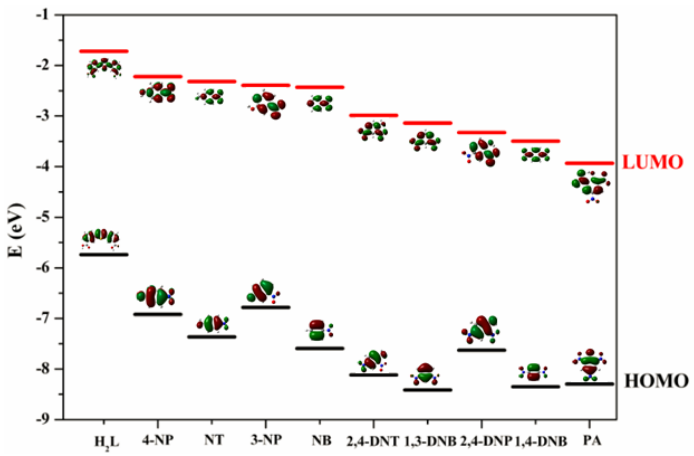

Fig. S26 HOMO and LUMO of H_2L ligand and explosive analytes.

Table S3. Summary of quenching constants (K_{sv}) for **MOF-1** and **MOF-2** for the sensing of explosive analytes at room temperature.

Analytes	K_{sv} (M^{-1})	
	MOF-1	**MOF-2**
PA	2.40×10^4	2.46×10^4
2,4-DNP	1.22×10^3	1.01×10^3
4-NP	7.25×10^2	6.97×10^2
NB	3.09×10^2	2.31×10^2
NT	3.96×10^2	2.79×10^2
1,3-DNB	4.26×10^2	2.94×10^2
1,4-DNB	6.03×10^2	5.70×10^2
2,4-DNT	4.92×10^2	2.73×10^2
3-NP	3.91×10^2	2.94×10^2

Table S4. HOMO and LUMO energies calculated for H_2L ligand and explosive analytes at B3LYP/6-31G* level.

Analytes	HOMO (eV)	LUMO (eV)	Band gap (eV)
H_2L	-5.7396	-1.7187	4.0209
4-NP	-6.9210	-2.2210	4.7000
NT	-7.3646	-2.3178	5.0468
3-NP	-6.7814	-2.3930	4.3884
NB	-7.5927	-2.4294	5.1633
2,4-DNT	-8.1181	-2.9877	5.1304
1,3-DNB	-8.4151	-3.1376	5.2775
2,4-DNP	-7.6284	-3.3253	4.3031
1,4-DNB	-8.3519	-3.4964	4.8555
PA	-8.2976	-3.9326	4.3650

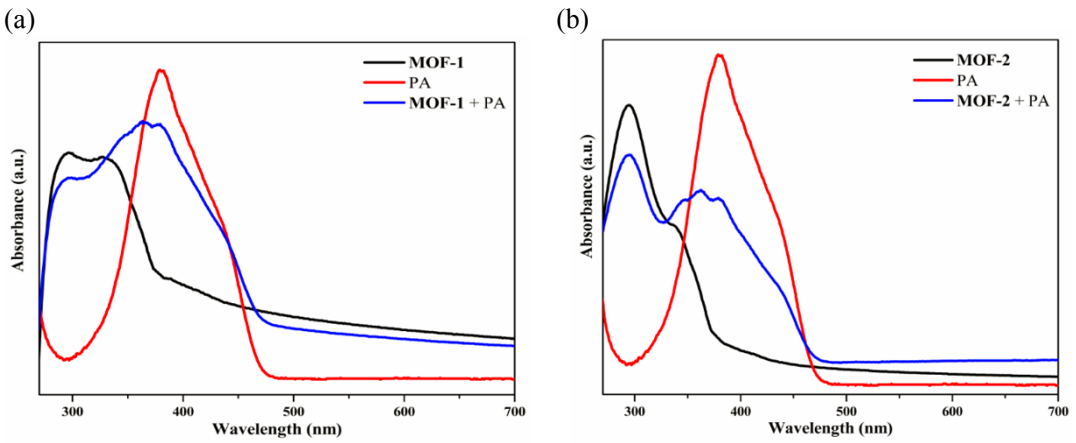

Fig. S27 UV-Vis spectra of **MOF-1** (a) and **MOF-2** (b) in DMA and upon addition of PA.

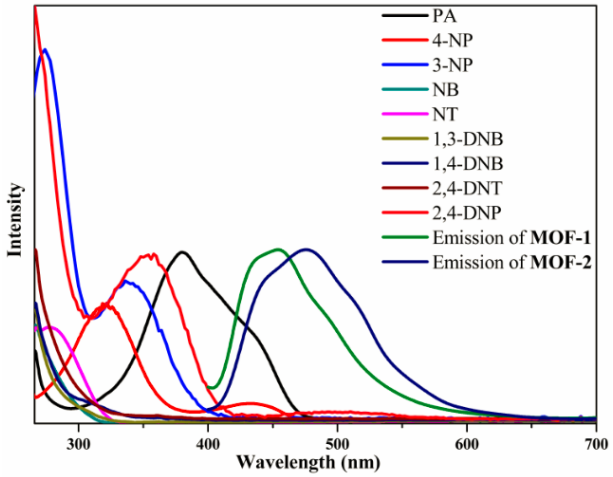

Fig. S28 Spectral overlap between normalized absorbance spectra of explosive analytes and the normalized emission spectra of **MOF-1** and **MOF-2** in DMA.

References

1 Bruker 2000, *SMART (Version 5.0), SAINT-plus (Version 6), SHELXTL (Version 6.1), and SADABS (Version 2.03)*, Bruker AXS Inc., Madison, WI.

2 A. L. Spek, Platon Program, *Acta Crystallogr*., *Sect*. *A*: *Fundam. Crystallogr*., 1990, **46**, 194.

3 V. A. Blatov, A. P. Shevchenko, V. N. Serezhkin, *J. Appl. Crystallogr*., 2000, **33**, 1193.